Electrically driven hybrid instabilities in smectic C liquid crystal films.

STEFAN RIED[1], HARALD PLEINER[1], AND WALTER ZIMMERMANN[2]

[1] *Max–Planck–Institute for Polymer Research, D-55021 Mainz, Germany*
[2] *Theoretische Physik, University of the Saarland, D-66041 Saarbrücken, Germany*

Abstract. – Novel static hybrid instabilities in smectic C liquid (SmC) crystal films are described. The Frederiks transition, well known for nematic liquid crystals, also takes place in smectic C layers, but here it is spatially periodic and coupled to undulations of the smectic layer. The Helfrich–Hurault undulational instability, typical for smectic A liquid crystals, occurs in SmC liquid crystals too, but the wave vector of the undulation of the layers is oblique to the applied external field. In addition, this modified Helfrich–Hurault instability not only involves layer undulations, but also contains deformations of the director field, which are typical for the Frederiks transition. The coupled deformations depend on all three coordinate axis, thus characterizing 3–dimensional patterns. There are parameter ranges, where both types of static instabilities, which differ by the spatial wavenumber, compete with each other near codimension–2 bifurcations.

Introduction. – Instabilities in liquid crystals have a long history and are very important in liquid crystal displays, for studying material properties as well as for nonlinear physics and pattern formation. Due to the additional liquid crystalline degrees of freedom they can be driven out of equilibrium not only by temperature or pressure gradients, or by imposed external flow, but also by external electric and magnetic fields. This allows for completely new instability mechanisms as well as for complex instability scenarios even for the first instabilities. The additional advantage of using free standing smectic liquid crystal films lies in their superior visualization properties and to explore new geometries in the experimental setup. For a long time instabilities in nematics on one hand, and those in smectic A on the other, have been explored separately. The nematic instabilities comprise the static and technological important Frederiks transition, a reorientation of the director under the influence of an external field, as well as the dynamic shear and electroconvective instabilities. In smectics A the undulational instability has found most interest, although others have also been considered. Of course, for instance the Bénard, the Marangoni and the Taylor instabilities are already known in simple liquids but they are modified and enriched by the additional liquid crystalline degrees of freedom (examples, overviews and references can be found in [1]).

Typeset using EURO-TₑX

Here we discuss theoretically the combined or hybridized instabilities of nematic and smectic types. They can occur in systems that show both kind of crystalline degrees of freedom, like smectic C or C* phases. A smectic C liquid crystal corresponds to a two–dimensional nematic, if the layers are fixed. Here the standard nematic instabilities, Frederiks transition and electroconvection, can be expected. In addition, rotating mechanical [2] and electrical fields [3] give rise to interesting target and spiral wave patterns. In the chiralized version, smectic C*, an in–plane polarisation exists rendering the in–plane system ferroelectric–like. If the twist (the polarization helix) is suppressed or negligible as in very thin films, the polarisation exists globally and allows for new coupling effects to an external electric field. This leads to new features in the Frederiks instability (like restabilization or hysteresis effects [4]), in electroconvection to a subharmonic regime [5] and to target waves in a rotating electric field [6, 7]. An external electric field can also undulate the layers due to the dielectric anisotropy (Helfrich–Hurault effect [8]) and both, nematic and smectic–type of instabilities come together. Due to the complexity of the equations involved to describe such hybridized instabilities this analysis is mostly numerical [9]. In this work we focus on an approximate analytical description of static instabilities neglecting electroconvection, which is an appropriate approach for clean samples (without free charges), for high frequencies of the driving field or for samples with a large negative electric conductivity anisotropy.

Basic Equations. – In liquid crystals a few continuous symmetries are spontaneously broken and the related hydrodynamic fields are used as additional macroscopic degrees of freedom [10]. In the nematic phase the rotational symmetry is spontaneously broken due to the orientational ordering of the molecules. The preferred mean direction is described by the director field $\hat{\boldsymbol{n}}(\boldsymbol{r}, t)$, with the constraint $\hat{\boldsymbol{n}}^2 = 1$ and the symmetry $\hat{\boldsymbol{n}} = -\hat{\boldsymbol{n}}$. In smectic liquid crystals there is in addition a spontaneously broken translation symmetry along one direction leading to a layered structure with a the density modulation along the layer normal $\hat{\boldsymbol{k}}(\boldsymbol{r}, t)$ ($|\hat{\boldsymbol{k}}| = 1$). Within the layers a smectic A phase is like an isotropic liquid and with the 'phase' variable $\phi(\boldsymbol{r}, t)$ the layers are numbered (it is integer in the middle of each layer). The true equilibrium state consists of flat, equidistant layers, where the layer normal $\hat{\boldsymbol{k}}$ is parallel to the z-axis and $\phi_{flat} = z$. For small deformations of flat layers it is convenient to introduce a displacement field (along the layer normal) $u(\boldsymbol{r}, t)$, by $\phi = z - u$. Rotations of the layer normal $\delta\hat{\boldsymbol{k}}$ are then related to transverse gradients of the displacement u in linear order by

$$\delta\hat{k}_i = -(\delta_{ij} - \hat{k}_i\hat{k}_j)\nabla_j u \,. \tag{1}$$

In the smectic C phase (SmC) the director is tilted with respect to the layer normal

$$\cos\psi = \hat{\boldsymbol{k}} \cdot \hat{\boldsymbol{n}} = \text{const.} \quad \leftrightarrow \quad \hat{\boldsymbol{k}} \cdot \delta\hat{\boldsymbol{n}} - \hat{\boldsymbol{n}} \cdot \delta\hat{\boldsymbol{k}} = 0. \tag{2}$$

Thereby rotational symmetry within the layers is spontaneously broken and SmC is biaxial. Thus SmC combines both, a smectic degree of freedom (u) and one that is nematic-like [10],

$$n_3 = \hat{\boldsymbol{p}} \cdot \delta\hat{\boldsymbol{n}} \quad \text{with} \quad \hat{\boldsymbol{p}} = \frac{\hat{\boldsymbol{n}} \times \hat{\boldsymbol{k}}}{|\hat{\boldsymbol{n}} \times \hat{\boldsymbol{k}}|} \tag{3}$$

and which describes rotations of the director about the layer normal (thus conserving the tilt angle ψ). In Fig. 1 the geometry is illustrated. The external electric field, $\boldsymbol{E} = \hat{\boldsymbol{p}} E_0$, is applied perpendicular to both, the undistorted layer normal and the undistorted director.

Static distortions of the SmC structure subject to an external field are given by the free energy density [11, 12, 13]

$$f = -\frac{1}{2}\epsilon_1\,(\boldsymbol{E} \cdot \hat{\boldsymbol{n}})^2 - \frac{1}{2}\epsilon_2\,(\boldsymbol{E} \cdot \hat{\boldsymbol{k}})^2 - \frac{1}{2}\epsilon_3\,\boldsymbol{E}^2 - \epsilon_4\,(\boldsymbol{E} \cdot \hat{\boldsymbol{n}})(\boldsymbol{E} \cdot \hat{\boldsymbol{k}}) + \frac{1}{2}F_{ij}\,(\nabla_i n_3)(\nabla_j n_3)$$

$$+ \frac{1}{2} B \left(\nabla_z u \right)^2 + \frac{1}{2} T_{ijkl} \left(\nabla_i \nabla_j u \right) \left(\nabla_l \nabla_k u \right) + C_{ijk} (\nabla_i n_3)(\nabla_j \nabla_k u) , \qquad (4)$$

where the first four terms describe the dielectric coupling of the field to both, the layer normal and the director. The next term gives the orientational-elastic (generalized Frank) energy. In the second line there is the elastic distortion energy due to layer compression as well as layer bending and the static cross-couplings between director and layer distortions. According to the triclinic symmetry of smectics C, the material tensors F_{ij}, T_{ijkl}, C_{ijk} contain 4 (F_{11}, F_{22}, F_{33}, F_{13}), 6 ($C_1,...,C_6$), and 9 ($T_1,...,T_9$) coefficients, respectively. The explicit form of the tensors can be found in [13], whereby the F_{ij} are generalized elastic Frank constants [11].
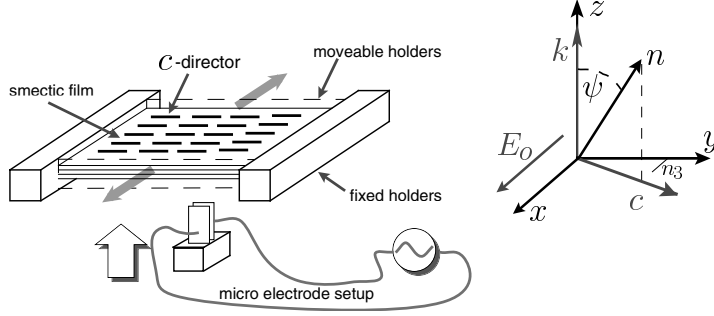

Fig. 1. – *Sketch of the geometry in the undistorted state. The $\hat{c}$-director is the projection of $\hat{n}$ onto the layers. In the undistorted state $n_3 = 0$.*

Stationary states are those that minimize eq. (4) for a given external field E_0. The linearized conditions for the extrema are

$$\left(\varepsilon_1 E_0^2 + F_{11} \partial_y^2 + F_{22} \partial_x^2 + F_{33} \partial_z^2 + 2F_{13} \partial_z \partial_y \right) n_3 = \qquad (5)$$
$$\left(\tilde{\varepsilon}_1 E_0^2 - \tilde{C}_1 \partial_z \partial_y - C_2 \partial_y^2 - \tilde{C}_3 \partial_z^2 - C_6 \partial_x^2 \right) \partial_x u ,$$

$$\left(- \tilde{\varepsilon}_1 E_0^2 + \tilde{C}_1 \partial_y \partial_z + C_2 \partial_y^2 + \tilde{C}_3 \partial_z^2 + C_6 \partial_x^2 \right) \partial_x n_3 = \Big(- \tilde{\varepsilon}_2 E_0^2 \partial_x^2 + B \partial_z^2 - T_1 \partial_z^4 \qquad (6)$$
$$- T_2 \partial_y^4 - T_3 \partial_x^4 - 6T_4 \partial_x^2 \partial_z^2 - 2T_6 \partial_y^2 \partial_z^2 - 2T_5 \partial_y^2 \partial_x^2 - 4\big(3T_7 \partial_x^2 + T_9 \partial_y^2 + T_8 \partial_z^2 \big) \partial_z \partial_y \Big) u ,$$

which will be solved for special cases in the following. We use the abbreviations $\tilde{C}_3 = C_3 + 2C_5$, $\tilde{C}_1 = 2(C_1 + C_4)$ and the effective dielectric anisotropies $\tilde{\varepsilon}_2 = \varepsilon_2 + 2\varepsilon_4 \cos \psi + \varepsilon_1 \cos^2 \psi$ and $\tilde{\varepsilon}_1 = \varepsilon_1 \cos \psi + \varepsilon_4$.

Boundary conditions. – We consider a smectic film confined between $z = \pm d/2$ either by two rigid plates or by air (free standing film). Accordingly, n_3 and u are fixed ("rigid" boundary conditions), or their thermodynamic conjugate force is zero ("free" boundary conditions). As indicated in Fig. 1, the electric field between the two electrodes (at $x = \pm L_x/2$) is along the x-direction. The electrodes can be in direct contact with the film (rigid b.c.) or separated by air (free b.c.). In any case, if the director or the layers are deformed periodically, the wavenumbers are discrete with characteristic step width of π/d and π/L_x for k_z and k_x, respectively. However, we will assume rather thin films and large electrode spacing, $d \ll L_x$, such that the minimally possible $k_{xc} \sim L_x^{-1}$ is small and k_x is (almost) continuous on the scale set by the minimal $k_{zc} \sim d^{-1}$. The y-direction is assumed to be infinite, so any distortion along that direction can show a continuous wave vector k_y.

Frederiks transition. – The anisotropies in the dielectric (and diamagnetic) susceptibilities lead to an orientation of the nematic director in external fields. In thin cells the competition between this field–driven orientation and the director orientation induced by container boundaries leads to the so–called Frederiks transition, which is well known since the early days of liquid crystals research [12, 14]. This orientational transition is crucial for the functioning of modern liquid crystal displays [15]. In order to see how the reduced symmetry of the smectic C phase (compared to nematics) can influence the Frederiks transition, we will assume, for the moment, fixed layers ($u \equiv 0$ with $C_i = 0 = \tilde{\epsilon}_1$). In that case eq. (5) reduces to

$$\left(F_{11}\,\partial_y^2 + F_{22}\,\partial_x^2 + F_{33}\,\partial_z^2 + 2\,F_{13}\,\partial_z\,\partial_y + \epsilon_1 E_0(t)^2\right) n_3 = 0 \; . \tag{7}$$

This equation reflects the reduced symmetry of the SmC phase, requiring that all equations are invariant under the replacement $x \to -x$, but only under the combined replacement $(y, z) \to (-y, -z)$.

Considering the stability of the ground state $n_3 = 0$ we make the mode ansatz according to the triclinic symmetry SmC liquid crystals

$$n_3 = \Big[n_{3,c}\cos(k_y y)\,\cos(k_z z) + n_{3,s}\sin(k_y y)\,\sin(k_z z)\Big]\cos(k_x x)\,. \tag{8}$$

Ansatz (8) leads to the wavenumber dependent expression for the critical electric field

$$E_{fred\,\pm}^2 = \frac{1}{\epsilon_1}\left(F_{11}k_y^2 + F_{22}k_x^2 + F_{33}k_z^2 \pm 2F_{13}k_y k_z\right)\,. \tag{9}$$

The true threshold is found by minimizing (9) with respect to k_y and k_x. This leads to the critical wavenumber $k_{yc} = \pm k_{zc}\,F_{13}/F_{11}$, where $k_{zc} = O(\pi/d)$ due to the boundary conditions at the top and the bottom of the film. For k_x the minimum value would be zero, but the finite electrode spacing requires $k_{xc} = \pi/L_x$ for fixed boundary conditions. For the geometry considered ($d \ll L_x$) $k_{xc} \ll k_{zc}$ the threshold field is then given by

$$E_{fred,c}^2 = \frac{1}{\epsilon_1}\frac{\pi^2}{d_z^2}\left(F_{33} - \frac{F_{13}^2}{F_{11}}\right) + \frac{1}{\epsilon_1}\frac{\pi^2}{L_x^2}F_{22} \tag{10}$$

where the second contribution is negligible for $d/L_x \to 0$. This (almost) 2-dimensional solution is due to the reduced symmetry in SmC allowing for a non-zero coefficient F_{13} unknown in nematics (with $F_{33}F_{11} - F_{13}^2 > 0$ for thermodynamic reasons). But (8) does not exactly fit the boundary conditions at the top and the bottom (neither fixed nor free ones), therefore formula (10) only gives the right order of magnitude of the threshold. In addition the approximation of fixed layers (all cross–couplings to undulations omitted) is used in this section but essentials features of Frederiks instability survive cross–coupling as described below.

Undulations. – In the opposite special case the director is kept fixed (i.e. $n_3 = 0$) but the layers can be distorted. An external field tends to reorient the layer normal according to the dielectric anisotropy. Since the layers cannot rotate homogeneously, they undulate and create regions, where the layer normal is rotated. This is the so–called Helfrich–Hurault instability [8] in SmA, which happens if the electric field is strong enough to overcome the elastic and orientational–elastic energy involved. Neglecting the coupling with n_3 (i.e. $C_i = 0 = \tilde{\epsilon}_1$) the state is determined by eq. (4). Using a simplified two-mode ansatz for u similar as for n_3 in eq. (8), the threshold condition for undulations as it follows from eq. (6) is of the form

$$\begin{aligned}
E_{und\pm}^2 &= \frac{1}{k_x^2\,\tilde{\epsilon}_2}\Big[Bk_z^2 + T_1 k_z^4 + T_2 k_y^4 + T_3 k_x^4 + 6T_4 k_x^2 k_z^2 + 2T_6 k_y^2 k_z^2 + 2T_5 k_x^2 k_y^2 \\
&\quad \pm 4\left(3T_7 k_x^2 + T_9 k_y^2 + T_8 k_z^2\right)k_y k_z\Big]\,.
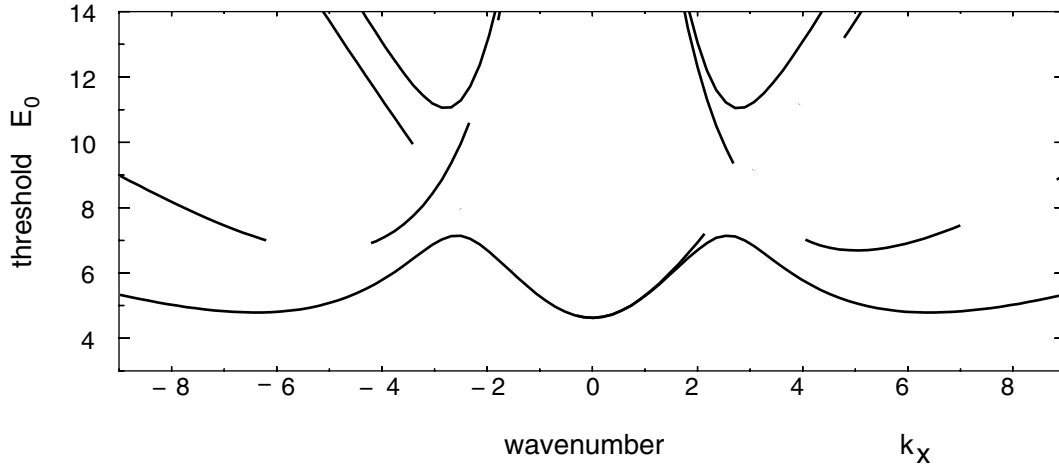\end{aligned} \tag{11}$$

Fig. 2. – Neutral curves as function of the wavenumber k_x for different solutions: The dashed line shows $E_{und-}(k_x)$ for eq. (11), the dash-dotted line $E_{fred-}(k_x)$ for eq. (9), while the upper and lower solid lines show $E_{hyb\pm2}(k_x)$ of eq. (15), respectively. The following parameters have been used: $k_y = k_z = 0.8$, $F_{11} = 1$, $F_{22} = 0.4$, $F_{33} = 3$, $F_{13} = 1$, $C_i = 0.5$, $T_i = 1$, $\varepsilon_1 = 0.06$, $\varepsilon_2 = 1$, $\varepsilon_4 = 0$.
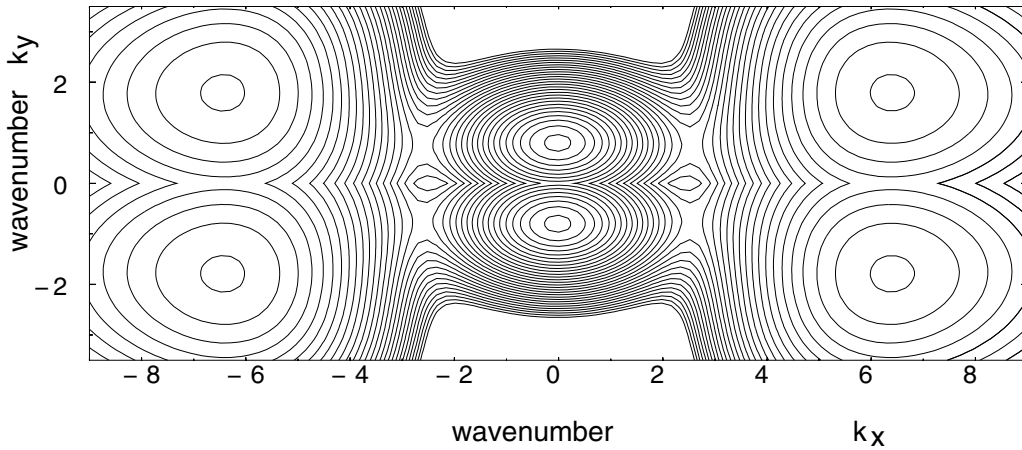
Fig. 3. – The neutral surface $E_{hyb}(k_x, k_y)$ according to equation (15) is shown; in particular $E_{hyb-2}(k_x, k_y)$ for $k_y > 0$ and $E_{hyb-1}(k_x, k_y)$ for $k_y < 0$ ($k_z = 0.8$), which show three minima each (inside the circles). The material parameters are as in Fig. 2.

The expression E^2_{und-} corresponds to the lower threshold and has generally four minima with different (nonzero) values for the wavenumber components k_{xc} and k_{yc}. This four–fold degeneracy is similar to the oblique–roll instability in electroconvection in nematics [16, 1], although in the latter system the different spatial patterns are due to a spontaneous symmetry breaking at the threshold, while in the present system they are due to the SmC symmetry. The corresponding patterns are the two independent real modes $\cos(k_{xc_{1,2}}x + k_{yc_{1,2}}y + \phi_{1,2})\cos(k_z z)$, which depend on all three spatial dimensions. A graphical representation of $E^2_{und-}(k_x)$ is shown by the dashed line in Fig. (2).

Hybrid Instabilities. – In the two preceding sections we have discussed the two instability

mechanisms individually by setting the cross–coupling terms in the free energy expression to zero. Lifting these artificial constraints the two degrees of freedom are coupled and the appropriate instabilities get hybridized. That means in smectic C liquid crystals the undulational instability is no longer a matter of layer deformations only, but is also accompanied by director reorientations and, vice versa, the Frederiks instability involves layer deformations, too.

In order to get realistic threshold conditions one may expand the two fields u and n_3 into a set of functions that match the boundary conditions. The threshold condition that arises after an appropriate truncation of such an expansion usually is too high in dimension as to be treated analytically, but standard methods are available. These numerical results (including dynamic aspects) [9] will be reported elsewhere. However, it turns out that a much simpler ansatz of two modes for each variable, cf. eq.(8), already covers the main features of the SmC symmetry including the cross–coupling and the main results qualitatively, although the boundary conditions are again not taken into account exactly. Inserting such a 2x2-mode ansatz into eqs. (5,6) results in four homogeneous coupled equations and therefore in the implicit threshold condition for E_0^2

$$\Delta_+^{(f)}\Delta_-^{(f)}\Delta_+^{(u)}\Delta_-^{(u)} + S_+^2 S_-^2 - S_+^2\Delta_-^{(f)}\Delta_-^{(u)} - S_-^2\Delta_+^{(f)}\Delta_+^{(u)} = 0 \tag{12}$$

with

$$\Delta_\pm^{(f)} = \epsilon_1(E_0^2 - E_{fred\pm}^2), \qquad \Delta_\pm^{(u)} = \tilde{\epsilon}_2 k_x^2 (E_0^2 - E_{und\pm}^2), \quad \text{and} \quad S_\pm = k_x\tilde{\epsilon}_1(E_0^2 + \hat{C}_\pm), \tag{13}$$

where $E_{fred\pm}^2$ and $E_{und\pm}^2$ are given by eq. (9) and (11), respectively, and where

$$\hat{C}_\pm = C_2 k_y^2 + \tilde{C}_3 k_z^2 + C_6 k_x^2 \pm \tilde{C}_1 k_y k_z. \tag{14}$$

Eq. (12) has the solutions $S_\pm^2 = \Delta_\pm^{(f)}\Delta_\pm^{(u)}$ which can be solved for the threshold fields of the hybrid instabilities ($\bar{\epsilon}^2 \equiv \epsilon_1\tilde{\epsilon}_2 - \tilde{\epsilon}_1^2 = \epsilon_1\epsilon_2 - \epsilon_4^2$)

$$E_{hyb\pm1,2}^2 \;\; = \;\; \frac{1}{2\bar{\epsilon}^2}\left[G_{1,2} \pm (G_{1,2}^2 - 4\bar{\epsilon}^2 H_{1,2})^{1/2}\right] \tag{15}$$

with

$$G_{1,2} = \epsilon_1\tilde{\epsilon}_2\left(E_{fred\pm}^2 + E_{und\pm}^2\right) + 2\tilde{\epsilon}_1\hat{C}_\pm \quad \text{and} \quad H_{1,2} = \epsilon_1\tilde{\epsilon}_2 E_{fred\pm}^2 E_{und\pm}^2 - \tilde{\epsilon}_1^2\hat{C}_\pm^2, \tag{16}$$

where the subscripts $\{1,2\}$ refer to the $\{$upper, lower$\}$ signs in the subscripts of E_{fred}^2, E_{und}^2 and $\hat{C}$. Due to the coupling the thresholds for undulations (dashed line in Fig. 2) and for director distortions (dash–dotted line in Fig. 2) are replaced by the threshold of the hybrid instabilities (solid lines in Fig. 2 for $E_{hyb\pm2}$). The threshold for the lowest branch E_{hyb-2} (for $k_y > 0$) and E_{hyb-1} (for $k_y < 0$) is shown as a function of the wavenumbers k_x and k_y in Fig. 3. According to this hybridization there is now a certain parameter range where six minima of $E_{hyb-1,2}$ are degenerated and have the same value as indicated in Fig. 3. Hence, there may be a competition between the three related modes $\propto A_{und_{1,2}}\cos(k_{xc_{1,2}} + k_{yc_{1,2}}y + \phi_{und_{1,2}})$ or $\propto B_{fred}\cos(k_{yc_3}y + \phi_{fred})$. However, only their nonlinear interaction beyond threshold decides about a competition or a possible coexistence, whereby in the latter case interesting patterns may occur beyond threshold. The branch E_{hyb+1} is not displayed, which leads always, similar as E_{hyb+2}, to higher thresholds than the lowest ones shown in Fig.3.

Conclusion. – We have discussed theoretically the hybridization of the electrical field driven Frederiks and undulation instabilities in smectic C liquid crystal films. Both types of instabilities mix director reorientation and layer undulations. Nevertheless essential features of each instability survive the hybridization as indicated in Fig. 2. In SmC both instabilities now

occur simultaneously accompanied by a competition between each other near codimension–2 points, which may give rise to interesting patterns beyond threshold. The patterns obtained by linear stability analysis are 3–dimensional reflecting the low symmetry of SmC phases. Our analytical treatment with a simplified 4–mode ansatz covers the SmC symmetry and leads to a qualitatively correct picture when compared to a multi–mode approach (with correct boundary conditions) that has to be solved numerically [9]. The advantage of this truncated ansatz is that it allows to write down analytically the qualitatively correct threshold, which is of great value for further exploration of the huge parameter space.

We have omitted the possibility of layer buckling, where the film as a whole is bent transversely (in contrast to undulations, where the first and last, or the middle, layer is kept flat). This is justified for fixed boundaries at the top and bottom (which sometimes is realized in systems having a more complicated structure than SmC in the first and last layers). For truly free standing films, this instability type can also take part in the hybridization [9], but for a large parameter range it does not change the general picture described here. We have also refrained, for lack of space, from discussing electro-hydrodynamic instabilities within the layers. They also show 3-dimensional flow and director patterns [9], but are relevant only for dirty systems (carrying charges) with positive (or only moderate negative) electric conductivity anisotropy.

<center>***</center>

<center>***</center>

REFERENCES

[1] *Evolution of Spontaneous Structures in Dissipative Continuous Systems*, eds. F.H. Busse and S.C. Müller (Springer, 1998); *Pattern Formation in Liquid Crystals*, eds. A. Buka and L. Kramer (Springer, 1995); *Nonlinear Physics of Complex Systems*, eds. J. Parisi, S.C. Müller and W. Zimmermann (Springer, 1996).

[2] P.E. Cladis, Y. Couder, and H.R. Brand, *Phys. Rev. Lett.* **55**, 2945 (1985).

[3] P.E. Cladis, P.L. Finn, and H.R. Brand, *Phys. Rev. Lett.* **75**, 1518 (1995).

[4] W. Zimmermann, S. Ried, H. Pleiner, and H.R. Brand, *Europhys. Lett.* **33**, 521 (1996).

[5] S. Ried, H. Pleiner, W. Zimmermann, and H.R. Brand, *Phys. Rev.* **E53** , 6101 (1996).

[6] F. Kremer, S.U. Vallerien, H. Kapitza, and R. Zentel, *Phys. Lett.* **A146**, 273 (1990).

[7] G. Hauck and H.D. Koswig, *Ferroelectrics*, **122**, 253 (1991).

[8] H. Helfrich, *Appl. Phys. Lett.* **17**, 531 (1970) and J.P. Hurault, *J. Chem. Phys.* **59**, 2068 (1970).

[9] S. Ried, Elektrisch getriebene Konvektion in smektischen Filmen, PhD Thesis, Universität Essen, (Shaker Verlag [http://www.shaker.de], ISBN 3-8265-3792-0, 1998).

[10] P.C. Martin, O. Parodi, and P. Pershan, Phys. Rev. **A6**, 2401 (1972).

[11] A. Saupe, Mol. Cryst. Liq. Cryst. **7**, 59 (1969).

[12] P. G. de Gennes and J. Prost, *The Physics of Liquid Crystals* (Clarendon, Oxford, 1993).

[13] H. Pleiner and H.R. Brand, Physica A **265**, 62 (1999).

[14] V. Frederiks and V. Tsvetkov, Sov. Phys. **6**, 490 (1934).

[15] B. Bahadur, *Liquid Crystals, Applications and Uses* (World Scientific, Singapore, 1993).

[16] W. Zimmermann and L. Kramer, *Phys. Rev. Lett.* **55**, 402 (1985).